

# Wave-current interaction with Boussinesq approaches

Florent GUINOT

*IFREMER, Brest, FRANCE*

**ABSTRACT:** Two numerical tools have been developed to model the propagation and interaction of waves and current over variable bathymetry in order to study the global kinematics on the whole fluid. The first one is a high-order Boussinesq model which can model irrotational waves and current in deep and shallow water with highly accurate kinematics and nonlinear properties. The other is based on a rotational Boussinesq formulation which can handle waves over rotational current but only in shallow water. The paper will briefly show what is behind these two approaches, the accuracy and limitations of both formulation and different results.

## 1 INTRODUCTION

### 1.1 *Context of the work*

Different kinds of tidal stream energy converter, which use the kinematical energy of the current, have been developed recently. Conventional studies to apprehend the real production and estimate the survivability of the system have (almost) always been done assuming an incident flow uniform and stationary. But real marine conditions are much more complex with the presence of waves and varying bathymetry. Some very recent studies have shown the importance of using more realistic marine flow conditions to study current turbines. For example the non-uniformity of the current profile, the turbulence induced mainly by bottom interaction as well as the unstationary motions due to waves will greatly affect the loadings and the performance of the system. Thus it is necessary to well describe what is really happening inside the fluid to give realistic inputs for current turbines studies and this paper is part of this more general work.

### 1.2 *The Boussinesq approach*

The idea in Boussinesq formulations is to eliminate the vertical coordinate from the classical Euler equations in order to reduce the computational effort. For example the original formulation (Boussinesq, 1872) assumed a horizontal velocity uniform over depth. This kind of approximation is inevitably limited to shallow water and weakly nonlinear problem. But during the last 20 years major improvements have been done in Boussinesq modelling and now the shallow water limitation can be overstep and many different phenomena can be simulated accurately like wave-wave interaction (Madsen et al. 2003), wave blocking by an opposite current (Guinot et al. 2007), propagation over rapidly varying bathymetry (Madsen et al. 2006)...

## 2 THE GOVERNING EQUATIONS

Both formulation will be described in two dimensions for simplicity but can directly be extended to 3D. A Cartesian coordinates system  $(x,z)$  is used with the  $z$ -axis pointing positive upwards. The fluid domain is bounded by the seabed at  $z=-h(x)$  and the free surface at  $z=\eta(x,t)$ . The still water level is located at  $z=0$ . The subscripts  $h$ ,  $\eta$ ,  $0$  or  $z$  respectively denotes variables taken at the related altitude.

### 2.1 The high-order Boussinesq formulation

For a full description of this formulation the reader is referred to Furhman (2004). Here only the general idea of the development is given.

The fluid is assumed incompressible, inviscid and irrotational. An exact solution to the Laplace equation,  $\Delta\phi=0$ , can be expressed as :

$$u(x,z,t) = \cos(z\nabla) u_0 + \sin(z\nabla) w_0 \quad (1)$$

$$w(x,z,t) = \cos(z\nabla) w_0 - \sin(z\nabla) u_0 \quad (2)$$

Where the *cos* and *sin* operators are infinite Taylor series operators defined by :

$$\cos(z\nabla) = \sum_{n=0}^{\infty} (-1)^n \frac{z^{2n}}{(2n)!} \nabla^{2n} \quad \sin(z\nabla) = \sum_{n=0}^{\infty} (-1)^n \frac{z^{2n+1}}{(2n+1)!} \nabla^{2n+1}$$

Yet the accuracy of the velocity profile can be improved by generalizing the previous expansion to an arbitrary  $z$ -level which is assumed to be a constant fraction of the sea bed,  $\hat{z} = -\sigma h$ ,  $0 \leq \sigma \leq 1$  (typical value is  $\hat{z} = -0.5h$ ).

From (1) and (2), the velocity variable taken at  $\hat{z}$  (denoted  $\hat{u}$  and  $\hat{w}$ ) are expressed as a function of  $u_0$ ,  $w_0$  and  $\hat{z}$ . By successive inversion  $u_0$  and  $w_0$  can be expressed as a function of  $\hat{u}$  and  $\hat{w}$  and then by substitution into (1) and (2),  $u$  and  $w$  can be expressed from  $\hat{u}$  and  $\hat{w}$  (see Madsen et al. 2002, for full development). Then this infinite expansion has to be truncated to be treated from a numerical point of view and further improvements can be achieved by using a new expansion from new variables involving Padé approximations.

### 2.2 The rotational formulation

This formulation is based on Shen (2000) who has suggested a way to model waves over rotational current but hasn't implemented it for surface gravity waves. A similar approach can be found in Rego et al. (2001) who didn't present any numerical results and in Veeramony et al. (2000) but their work was only focused on wave breaking. The idea is to solve a Poisson equation obtained by mixing the continuity equation  $\nabla u + \partial w / \partial z = 0$  and the  $y$ -axis component of the vorticity vector (expressed here in a dimensionless form)

$$s_y = \partial u / \partial z - \mu^2 \partial w / \partial x \quad (3)$$

The Poisson equation can be written as :

$$\partial^2 w / \partial z^2 + \mu^2 \nabla^2 w = -\partial s_y / \partial x \quad (4)$$

Following a more classical Boussinesq approach,  $u$  and  $w$  are expanded in the form  $u = u_0 + \mu^2 u_1 + O(\mu^4)$ . Inserting these expansions into (3) and (4), we get a system of equations which can be solved using the bottom boundary condition, the continuity equation expressed at an intermediate depth  $\hat{z} = -\sigma h$  and the value of  $u$  at  $\hat{z}$  as boundary conditions.

### 2.3 The fully nonlinear time-stepping problem

The time evolution of the problem is governed by the usual kinematic and dynamic free surface boundary conditions written in this more common form:

$$\frac{\partial \eta}{\partial t} + U_\eta \cdot \nabla \eta - w_\eta (1 + \nabla \eta \nabla \eta) = 0 \quad (5)$$

$$\frac{\partial U_\eta}{\partial t} + g \nabla \eta + \frac{1}{2} \nabla (U_\eta^2 - \frac{w_\eta^2}{2} (1 + \nabla \eta \nabla \eta)) = 0 \quad (6)$$

With  $U_\eta = u_\eta + w_\eta \nabla \eta$ .

In two dimensions, these equations are the same for both the irrotational and the rotational formulation. In 3D new terms appear in the dynamic free surface condition (6) for the rotational formulation. Those additional rotational terms can be expressed as  $\mathbf{u}_\eta \times (\nabla \times \mathbf{U}_\eta)$  where the  $\times$  is the cross product and  $\mathbf{u}$ ,  $\mathbf{U}$  and  $\nabla$  are vectors containing their respective x and y components. Moreover for the rotational formulation the following vorticity equation has to be added to the time stepping problem:

$$Ds_y/Dt = 0 \quad (5)$$

## 3 ACCURACY AND LIMITATIONS OF BOTH APPROACH

From the Fourier analysis described in Madsen et al. 2003, the range of applicability of those systems of equations can be determinate for wave propagating on a mildly sloping bottom. As this study has already been done for the high-order formulation, only some key numbers will be given here to compare with the rotational formulation. The reader can referred to Madsen et al. 2003 or Furhman 2004 for the full description of the Fourier analysis and the accuracy and limitations of the high-order formulation.

### 3.1 Linear dispersion relation and Doppler shift

As it is one of the most fundamental property embedded in this system of equations, the linear dispersive properties has been examined first.

Stokes theory gives the well known dispersion relation for linear waves propagating over a uniform current:

$$(\omega - kU_0)^2 = gk \tanh(kh) \quad (6)$$

The Fourier analysis gives the following dispersion relations for each formulation.

High-order formulation:  $(\omega - kU_0)^2 = ghk^2(1+1/9k^2h^2+1/945k^4h^4)/(1+4/9k^2h^2+1/63k^4h^4)$

Rotational formulation:  $(\omega - kU_0)^2 = ghk^2(1-(\alpha+1/3)k^2h^2)/(1-\alpha k^2h^2)$

Where  $\alpha = \sigma + \sigma^2/2$ . The optimal value is  $\alpha = -0.390$  equivalent to  $\sigma = -0.531$ .

Figure 1 represents the solutions of these relations in terms of nondimensional wave number  $kh$  as a function of Froude number  $Fr = U_c / \sqrt{gh}$  for different water depths.

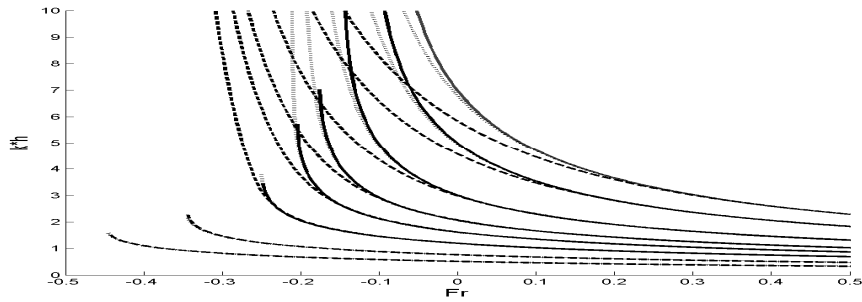


Figure 1. Comparison of dispersive property. Full lines, Stokes theory. Dash grey lines, High-order formulation. Dotted lines, rotational formulation. The relative water depth  $k_0 h = \omega^2 / g^* h$  is respectively from bottom to top [0.25; 0.5; 1; 1.5; 2; 3; 5; 7].

The end of each line represents wave blocking by an opposite current. We can see that the high-order formulation is extremely accurate except close to the blocking points of short waves. For the rotational formulation, even far from the blocking point a significant error appears from  $kh=4$ . The fact that for the models, some curves don't end at the blocking point implies that in these conditions even if some waves are propagating over an opposite current exceeding the theoretical value of blocking, the wave will continue to propagate with a wave length decreasing infinitely whereas normally, reflection should appear.

### 3.2 Shoaling properties

To quantify the shoaling accuracy of the formulations we used the linear shoaling gradient defined by :

$$\gamma = \frac{A_x}{A} \frac{h}{h_x}$$

Where A is the wave amplitude and h the water depth.

This should be compared to the reference solution (see Madsen et al. 2006):

$$\gamma = \frac{2kh \sinh(2kh) + 2k^2 h^2 (1 - \cosh(2kh))}{(2kh + \sinh(2kh))^2}$$

The lengthy expressions of the shoaling gradient will not be given here for brevity but the following graph shows the comparison between both formulations and the theory. Different curves are shown because the initial shoaling gradient for the rotational formulation is only accurate till  $kh=0.8$  (line with squares) which really limits the application of the model. Nevertheless by optimizing some coefficient in the original solution of the system (cf Madsen 2006 for detailed explanation of this kind of optimization), we allow a minor error for low values of  $kh$  ( $kh < 0.5$ ) in order to improve the accuracy afterwards. The two others curves presented are optimization for  $0 < kh < 2$  (line with crosses) and for  $0 < kh < 3$  (line with dots).

In the range of  $kh$  shown, the high-order formulation perfectly fits the theoretical solution (full line). Significant error appears around  $kh=30$ .

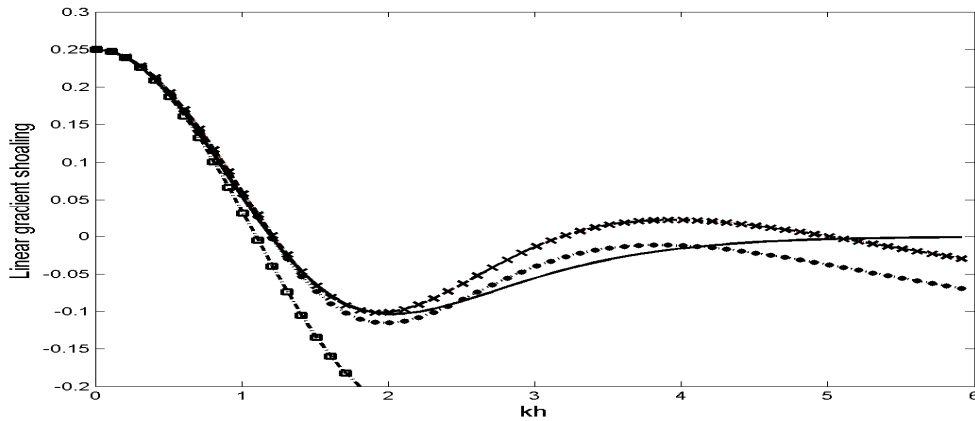


Figure 2. Linear shoaling gradient. Full line, theoretical solution and high-order formulation. Squares, original solution. Crosses, optimization for  $kh=[0\ 2]$ . Dots, optimization for  $kh=[0\ 3]$ .

### 3.3 Accuracy in velocity profile

As the final aim of these models is to represent some velocity profiles, the accuracy of both formulations has been studied. There are different ways to quantify the error in the velocity profile representation and the following depth-averaged error is used.

$$F_u(kh) = \sqrt{\frac{1}{h} \int_{-h}^0 \left( \frac{u(z)}{u(0)} - \frac{u_s(z)}{u_s(0)} \right)^2 dz}$$

Where  $u_s$  represents the velocity field from linear Stokes theory.

Figure 3 shows this depth-averaged error for the rotational formulation and an example of vertical profile of horizontal velocity under a wave crest for  $kh=4$ . In the range of  $kh$  shown, the high-order formulation error is extremely small. Significant error appears around  $kh=12$ .

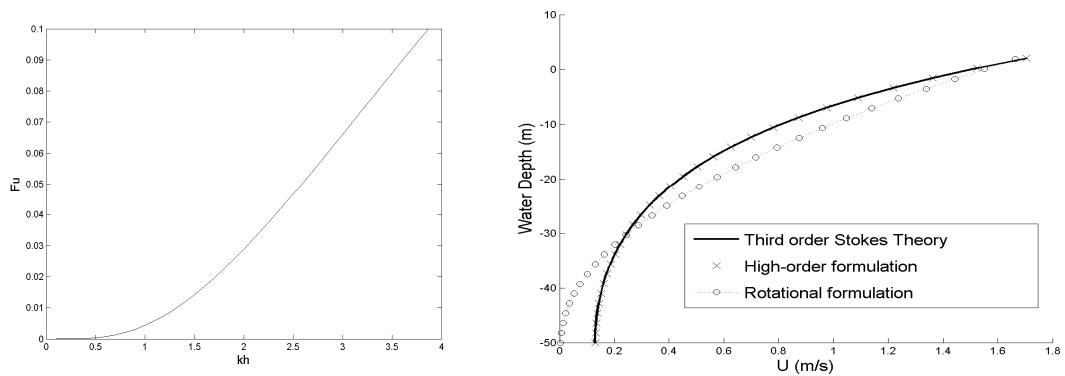


Figure 3. (Left) Velocity depth-averaged error for the rotational formulation. (Right) Velocity profile under a wave crest from third order Stokes theory (Full Line), high-order formulation (Crosses) and rotational formulation (Circles).

## 4 THE NUMERICAL MODEL

### 4.1 Numerical procedure

The numerical solution procedure is based on finite difference discretizations on a uniform grid. The time integration is done using an explicit fourth-order Runge-Kutta scheme. To maintain numerical stability in simulations involving vorticity or variable bathymetry, Savitzky-Golay smoothing filter is applied (most of the time an 8th-order, 11-point filter is used). The generation and absorption of waves and current are made using relaxation zones. In a first zone (one wave length long) a theoretical solution for waves, current and vorticity is implemented. Then a second zone does a smooth transition between the theoretical and the numerical solution (this zone also absorbs backward reflected waves). And at the end of the domain a zone equivalent to a sponge layer is used. This numerical procedure is similar to the one used by Furhman 2004 and a full description can be found there.

### 4.2 Wave blocking

A previous study (Guinot et al. 2007) have shown that wave blocking by an opposite current can be simulated accurately with the high-order formulation. Different test cases have been done to check the capability of the rotational model to simulate wave-blocking and as expected, in the range of applicability of the model, the blocking simulations are really similar to the ones with the high-order model. In the following example, the situation of the blocking point is the same for both models and the error from the theoretical value is around 2%.

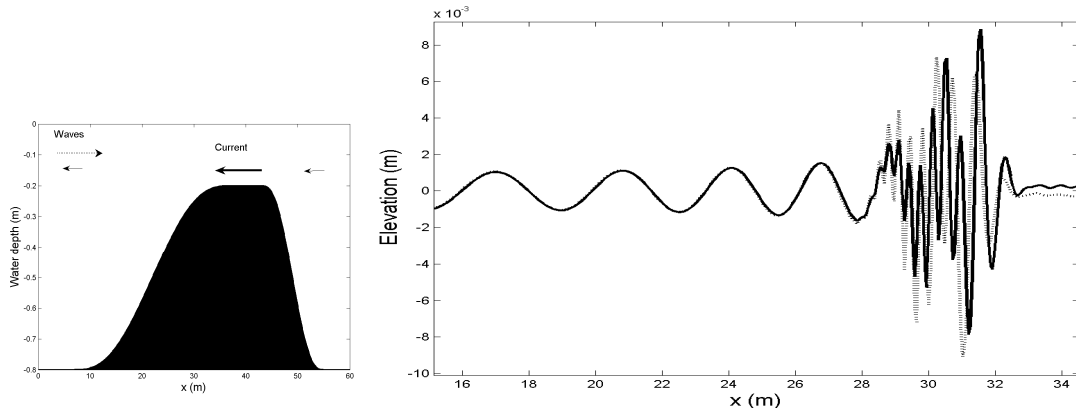


Figure 4. Simulation of wave blocking. Left, configuration used. Right, surface elevation after blocking from the high-order model (full line) and the rotational model (dotted line). The initial conditions are  $T=2s$ ,  $H=0.002m$ ,  $U_{current} = -0.17m/s$  at the border and  $-0.809$  on the top.

### 4.3 Waves over rotational current

Some simulations of waves propagating over a rotational current have been made. For the moment, as any viscous effects are present in the equations, there is no significant change in the current profile (as shown e.g. in Huang et al. 2003 ) but only a small decrease of the global current due to the backward current induced by the waves can be observed. The current profile and its relative vorticity are specified as an input in the model. Log law, power 1/7 and linearly sheared current have been tried. The only effect that can be seen yet is the change in wavelength of the incident waves compared to the same waves with a uniform current. A complete investigation is under going and will be published in a forthcoming publication but the first simulations are positive.

#### 4.4 Representation of the velocity field

With these two models we can represent, in their range of applicability, the global velocity field for complex wave-current flow interacting over variable bathymetry.

The next two figures show two different useful representations of the velocity field. The first one is a representation in space at a fixed time (from the high-order formulation) and the second one a representation at different time at a fixed location (from the rotational formulation, the red thin line represents the initial current profile).

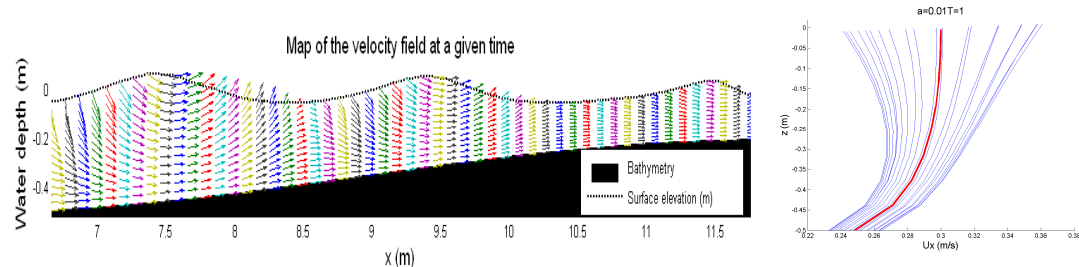


Figure 5. Two different examples of velocity field representation from each formulation.

## 5 CONCLUSION

Two different Boussinesq-type formulations with their own limitations and accuracy have been presented. The high-order formulation which represents the most efficient Boussinesq formulation by now is non-surprisingly extremely accurate for simulating wave and (uniform) current interaction. It represents a powerful tool to study the global kinematics of this kind of complex flow in shallow water as well as in deep water where the uniform current approximation becomes more realistic, at least in the main part of the water column. On the other side the rotational formulation, though much more limited than the previous one, seems to be a real breakthrough in the simulation of waves propagating over non-uniform currents especially with the direct possibility to include viscous effects into the vorticity terms.

## 6 REFERENCE

- FURHMAN D.R., 2004, Numerical solutions of Boussinesq equations for fully nonlinear and extremely dispersive water waves, *PhD Thesis, DTU*
- GUINOT, F., LE BOULLUEC M. & REY V., 2007. Interaction houle-courant en bathymétrie variable via une approche de type Boussinesq. *Proc. XI<sup>èmes</sup> Journées de l'Hydrodynamique*.
- HUANG Z. & MEI, C.C., 2003, Effects of surface waves on a turbulent current over a smooth or rough seabed, *Journal of Fluid Mechanics*, Volume 497, p. 253-287
- MADSEN P.A., BINGHAM H.B., LIU H., 2002, A new Boussinesq method for fully nonlinear waves from shallow to deep water, *J. Fluid Mech.*, vol. 462, pp. 1-30.
- MADSEN P.A., AGNON R. Y., 2003, Accuracy and convergence of velocity formulations for water waves in the framework of Boussinesq theory, *J. Fluid Mech.*, vol. 477, pp.285-319
- MADSEN P.A., FURHMAN D.R., WANG B., 2006, A Boussinesq-type method for fully nonlinear waves interacting with a rapidly varying bathymetry, *Coastal Engineering*, Volume 53, p. 487-504
- REGO, V.S. and NEVES, C.F., 2001, Nonlinear and dispersive waves on flows with horizontal vorticity, *Revista Brasileira de Recursos Hidricos*, 6
- SHEN C.Y., 2000, Constituent Boussinesq Equations for Waves and Currents, , *J. of Phys. Ocean.*, vol.31, pp.850-859
- VEERAMONY J. and SVENDSEN, I.A., 2000) The flow in surf-zone waves. *Coastal Engineering*, vol39, p. 93-122